Available online at www.sciencedirect.com
ScienceDirect
Journal of Magnetic Resonance 191 (2008) 148–155
JMR Journal of Magnetic Resonance
www.elsevier.com/locate/jmr

Commnication

Isotropic filtering using polyhedral phase cycles: Application to singlet state NMR

Giuseppe Pileio, Malcolm H. Levitt *

School of Chemistry, University of Southampton, University Road, Highfield, Southampton SO17 1BJ, UK

Received 14 November 2007
Available online 26 December 2007

Abstract

A technique is described for filtering out the components of an NMR signal that have passed through an isotropic spin order term. The method involves a coordinated cycle of three radiofrequency phase angles, where two of the phases correspond to the polar angles describing the vertices of a regular polyhedron, and the third angle is stepped around a circle. The most economical isotropic filtering scheme involves a 12-step phase cycle based on tetrahedral symmetry. The method is used to filter out NMR signals that have passed through singlet populations in a solution NMR experiment.

Keywords: Isotropic filtering; Singlet states; Long-lived spin states; Spherical tensor operators; Phase cycling

1. Introduction

Phase cycling is a ubiquitous method in NMR [1–9]. In general, signals are accumulated from many similar NMR pulse sequences, which differ only in the values of one or more radiofrequency phases. Linear superposition of the signals, multiplied by complex phase factors, is used to filter out classes of NMR signals with desirable properties, and to suppress undesired NMR signals or experimental artefacts. Techniques have been developed for designing phase cycles, based on an analysis of the coherence transfer pathways contributing to the NMR signals [1,2]. Many different phase cycling schemes have been designed, including nested phase cycles [1,2], cogwheel phase cycles [3–6] and multiplex phase cycles [7].

The coherence order of a spin order component describes its symmetry under rotations around a single axis, conventionally the static magnetic field axis (the laboratory frame z-axis). It is possible to extend this concept by classifying the nuclear spin order components according to their behavior under the full group of rotations in three-dimensional [8,9].

The natural language for a complete rotational classification is that of irreducible spherical tensor operators (ISTOs), since these span the irreducible representations of the full rotation group [10,11]. Irreducible spherical tensor operators are described by two quantum numbers, called the rank, denoted λ, and the component index μ, which takes $2\lambda+1$ values $\mu \in \{-\lambda, -\lambda+1, \ldots, +\lambda\}$. For spin operators, the component index of an irreducible spherical tensor operator corresponds to its quantum order, also known as the coherence order [1]. An ensemble of spin systems, each containing N coupled spins-1/2, can only support spin order terms for which both the rank λ and the quantum order μ are less than or equal to N.

The *isotropic spin order term* with $\lambda = \mu = 0$ is of particular interest since it is invariant to all three-dimensional rotations of the nuclear spin polarizations. Traditional phase cycles, which are based on the rotational properties of spin order terms around the z-axis, cannot distinguish this term from higher-rank components which also have $\mu = 0$. As described below, isotropic spin order is of particular interest in solution NMR, since it is a manifestation of

* Corresponding author. Fax: +44 23 8059 3781.
E-mail address: mhl@soton.ac.uk (M.H. Levitt).

1090-7807/$ - see front matter © 2007 Elsevier Inc. All rights reserved.
doi:10.1016/j.jmr.2007.11.021

singlet spin populations, which can have very long lifetimes in some circumstances [12–21].

The experimental classification of spin order terms according to the full rotation group was first demonstrated by Suter and Pearson, using a numerical fitting procedure [8]. A more concise closed solution, called *spherical tensor analysis* (STA), was developed recently [9] and applied to the study of endohedral hydrogen-fullerene complexes [22]. Spherical tensor analysis achieves a complete classification of the spin order terms according to both λ and μ, up to a known maximum rank. The experiment is very elaborate and requires the linear superposition of signals from a large number of independent experiments using different radiofrequency phases and complex weighting coefficients.

As discussed below, full STA is an overkill if only the isotropic component is required ($\lambda = \mu = 0$). In most cases the isotropic component of an NMR signal may be extracted using a phase cycle consisting of a relatively modest number of angles, and which may be derived from the vertices of a regular polyhedron. The choice of polyhedron depends on the maximum rank that needs to be taken into account for the spin system of interest, as shown in Table 1. If the maximum rank is 2, tetrahedral symmetry is sufficient, and the phase cycle involves 12 independent experiments. An application to singlet state NMR spectroscopy is described below.

2. Isotropic filtering

2.1. Implementation

The general scheme for *isotropic filtering* of an NMR signal is shown in Fig. 1. Suppose that a pulse sequence consists of two blocks, denoted A and B, with overall radiofrequency phases ϕ_A and ϕ_B. A reproducible initial state is established before block A and the complex NMR signal is detected in the interval after block B. In order to filter out the part of the NMR signal that passes through isotropic spin order at the junction of the two blocks, two strong $\pi/2$ pulses are inserted with phases ϕ_1 and ϕ_2 (Fig. 1b). Isotropic filtering is implemented by cycling the phases ϕ_A, ϕ_1, ϕ_2 and ϕ_B in $\mathcal{N}$ steps, where

$$\mathcal{N} = (\lambda_{\max} + 1)\mathcal{V} \tag{1}$$

Here $\lambda_{\max}$ is the highest rank of nuclear spin order with significant intensity at the junction of sequences A and B, and $\mathcal{V}$ is the number of vertices of a regular polyhedron chosen

Table 1
The type of polyhedron, the number of polyhedral vertices $\mathcal{V}$, and the number of phase cycle steps $\mathcal{N}$, required to implement isotropic filtering on a spin density operator with maximum spherical rank $\lambda_{\max}$

$\lambda_{\max}$	Polyhedron	$\mathcal{V}$	$\lambda_{\max}+1$	$\mathcal{N}$
2	Tetrahedron	4	3	12
3	Octahedron	6	4	24
4	Icosahedron	12	5	60
5	Icosahedron	12	6	72

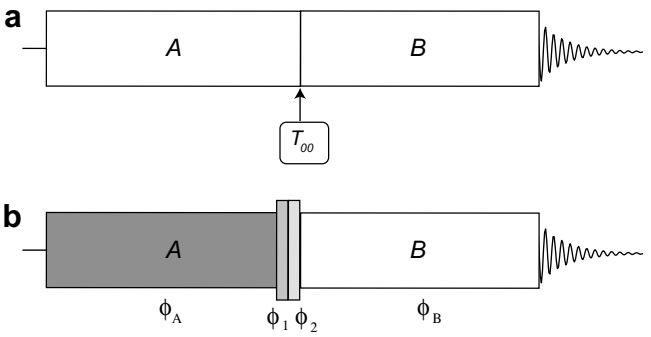

Fig. 1. General pulse sequence scheme for isotropic filtering of NMR signals. (a) Phase cycle consisting of two blocks, A and B, before isotropic filtering. (b) Isotropic filtering is implemented by inserting two $\pi/2$ pulses (small rectangles), with phase cycling of the phases ϕ_A and ϕ_B of the two blocks, and of the phases ϕ_1 and ϕ_2 of the two inserted pulses.

according to the value of $\lambda_{\max}$, as specified in Table 1. If $\lambda_{\max}$ is larger than 5, solutions based on the platonic solids no longer exist, and the Lebedev angle sets [9,23,24] may be used.

The radiofrequency phase angles for phase cycle step j are specified as follows. Consider the indices $j_1 \in \{0, 1, \ldots, \mathcal{V}-1\}$ and $j_2 \in \{0, 1, \ldots, \lambda_{\max}\}$, defined through

$$\begin{aligned} j_1 &= \mathrm{floor}\{j/(\lambda_{\max}+1)\} \\ j_2 &= j - j_1(\lambda_{\max}+1) \end{aligned} \tag{2}$$

where $\mathrm{floor}(x)$ is the largest integer that is not greater than x. The index j_1 counts through the $\mathcal{V}$ vertices of the polyhedron, while the index j_2 counts $\lambda_{\max}+1$ uniform steps around a circle, for each of these vertices. The radiofrequency phases are given by

$$\begin{aligned} \phi_A(j) &= \phi_A(0) + \phi_v(j_1) + \theta_v(j_1) + \frac{2\pi j_2}{(\lambda_{\max}+1)} \\ \phi_1(j) &= \phi_v(j_1) + \theta_v(j_1) \\ \phi_2(j) &= \phi_v(j_1) + \pi \\ \phi_B(j) &= \phi_B(0) \end{aligned} \tag{3}$$

where $\{\theta_v(j_1), \phi_v(j_1)\}$ are the polar angles defining the j_1th vertex of the regular polyhedron. The angles $\phi_A(0)$ and $\phi_B(0)$ are the base phases for the two pulse sequence blocks, which are determined by pulse sequence-specific considerations, independent of the phase cycling scheme.

The NMR signals for the $\mathcal{N}$ phase cycle steps are added together with the same weight. As shown below, this procedure projects out the part of the NMR signal that derives from isotropic spin order terms ($\lambda = \mu = 0$) in existence at the junction of the two pulse sequence blocks.

Explicit phase values for the cases $\lambda_{\max} = 2$ and 3 are given in Tables 2 and 3. Graphical representations of the phase values are shown in Fig. 2.

2.2. Theory

The NMR signal for step $j = 0$ in the phase cycle can be expressed as a superposition of *spherical signal*

Table 2
Rotational Euler angles $\{\alpha_j, \beta_j, \gamma_j\}$ and explicit radiofrequency phases $\{\phi_A, \phi_1, \phi_2, \phi_B\}$ for a 12-step tetrahedral phase cycle, suitable for isotropic filtering of an NMR signal with $\lambda_{\max} = 2$. The general pulse sequence scheme in Fig. 1 is used, assuming that the starting phases are $\phi_A(0) = \phi_B(0) = 0$. All angles are given in degrees

j	α_j	β_j	γ_j	$\phi_A(j)$	$\phi_1(j)$	$\phi_2(j)$	$\phi_B(j)$
0	0	0	0	0	0	180	0
1	0	0	120	120	0	180	0
2	0	0	240	240	0	180	0
3	0	109.47	0	109.47	109.47	180	0
4	0	109.47	120	229.47	109.47	180	0
5	0	109.47	240	349.47	109.47	180	0
6	120	109.47	0	229.47	229.47	300	0
7	120	109.47	120	349.47	229.47	300	0
8	120	109.47	240	109.47	229.47	300	0
9	240	109.47	0	349.47	349.47	60	0
10	240	109.47	120	109.47	349.47	60	0
11	240	109.47	240	229.47	349.47	60	0

Table 3
Rotational Euler angles $\{\alpha_j, \beta_j, \gamma_j\}$ and explicit radiofrequency phases $\{\phi_A, \phi_1, \phi_2, \phi_B\}$ for a 24-step octahedral phase cycle, suitable for isotropic filtering of an NMR signal with $\lambda_{\max} = 3$. The general pulse sequence scheme in Fig. 1 is used, assuming that the starting phases are $\phi_A(0) = \phi_B(0) = 0$. All angles are given in degrees

j	α_j	β_j	γ_j	$\phi_A(j)$	$\phi_1(j)$	$\phi_2(j)$	$\phi_B(j)$
0	0	0	0	0	0	180	0
1	0	0	90	90	0	180	0
2	0	0	180	180	0	180	0
3	0	0	270	270	0	180	0
4	0	90	0	90	90	180	0
5	0	90	90	180	90	180	0
6	0	90	180	270	90	180	0
7	0	90	270	0	90	180	0
8	90	90	0	180	180	270	0
9	90	90	90	270	180	270	0
10	90	90	180	0	180	270	0
11	90	90	270	90	180	270	0
12	180	90	0	270	270	0	0
13	180	90	90	0	270	0	0
14	180	90	180	90	270	0	0
15	180	90	270	180	270	0	0
16	270	90	0	0	0	90	0
17	270	90	90	90	0	90	0
18	270	90	180	180	0	90	0
19	270	90	270	270	0	90	0
20	0	180	0	180	180	180	0
21	0	180	90	270	180	180	0
22	0	180	180	0	180	180	0
23	0	180	270	90	180	180	0

components [8,9], each representing the part of the signal that passed through a spin order term with rank λ and quantum order μ, i.e.

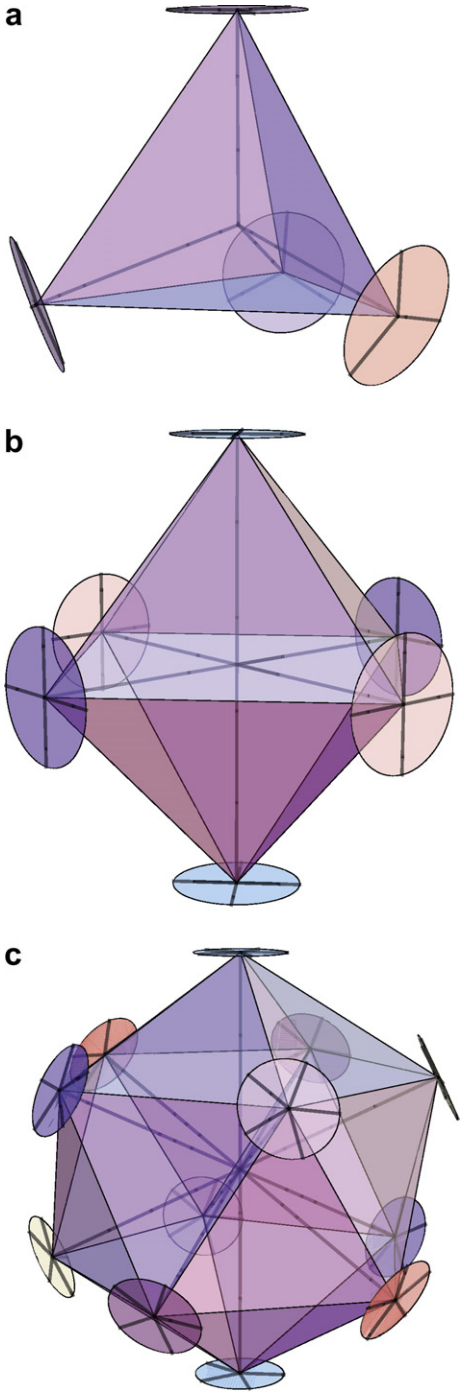

Fig. 2. Graphical representations of polyhedral phase cycles. The vertices of the polyhedra have polar angles $\{\theta, \phi\}$ given by the Euler angles $\{\beta_j, \alpha_j\}$. The values of the third Euler angle γ_j are represented by the spokes of a wheel attached to each vertex. (a) The 12-step tetrahedral phase cycle for $\lambda_{\max} = 2$. (b) The 24-step octahedral phase cycle for $\lambda_{\max} = 3$. (c) The 60-step icosahedral phase cycle for $\lambda_{\max} = 4$.

$$s(0,t) = \sum_{\lambda\mu} s_{\lambda\mu}(0,t) \tag{4}$$

The spherical components of the quadrature NMR signal are given in general by

$$s_{\lambda\mu}(0,t) = \sum_{\Lambda} (I^+ | \widehat{W}(t) \widehat{B} | T^{\Lambda}_{\lambda\mu})(T^{\Lambda}_{\lambda\mu} | \widehat{A} | \rho_0) \tag{5}$$

where the Liouville-space bracket [25] is defined $(A|B) = \mathrm{Tr}\{A^{\dagger}B\}$. Here ρ_0 is the initial spin density operator, $\widehat{A}$ is the superoperator for the first pulse sequence block, $\widehat{B}$ is the superoperator for the second pulse sequence block, and $\widehat{W}(t)$ is the time-dependent superoperator for the spin evolution during the signal detection period. The sum is taken over all spherical tensor operators $T^{\Lambda}_{\lambda\mu}$ with rank λ and quantum order μ. In general, there may be several such operators, which are distinguished by the label Λ.

The spherical tensor operators are defined by their transformation properties under rotations:

$$\widehat{R}(\Omega)|T^{\Lambda}_{\lambda\mu}) = \sum_{\mu'=-\lambda}^{+\lambda} D^{\lambda}_{\mu\mu'}(\Omega)|T^{\Lambda}_{\lambda\mu'}) \tag{6}$$

where $\widehat{R}(\Omega)$ is a rotation superoperator, Ω represents an Euler angle triplet $\Omega = \{\alpha, \beta, \gamma\}$ and $D^{\lambda}_{\mu\mu'}(\Omega)$ is a Wigner matrix element of rank λ. The rotation superoperator may be expressed in terms of the individual Euler rotations as follows:

$$\widehat{R}(\Omega) = \widehat{R}_z(\alpha)\widehat{R}_y(\beta)\widehat{R}_z(\gamma) \tag{7}$$

In many cases, the spherical signal components $s_{\lambda\mu}(0,t)$ are negligible for $\lambda > \lambda_{\max}$. In spin systems of finite size, this bound is rigorous. For example, in ensembles of independent systems, each containing N coupled spins-1/2, the spherical components $s_{\lambda\mu}$ vanish identically for $\lambda > N$.

The aim of isotropic filtration is to project out the isotropic signal component $s_{00}(0,t)$ from the total signal $s(0,t)$. This is achieved by performing a set of experiments in each of which a different rotation, described by the Euler angles $\Omega_j = \{\alpha_j, \beta_j, \gamma_j\}$, is inserted between the two pulse sequence blocks. The signal from the experiment with index j is given by

$$\begin{aligned} s(j,t) &= \sum_{\Lambda,\lambda,\mu} (I^{+}|\widehat{W}(t)\widehat{B}\widehat{R}(\Omega_j)|T^{\Lambda}_{\lambda\mu})(T^{\Lambda}_{\lambda\mu}|\widehat{A}|\rho_0) \\ &= \sum_{\Lambda,\lambda,\mu,\mu'} D^{\lambda}_{\mu\mu'}(\Omega_j)(I^{+}|\widehat{W}(t)\widehat{B}|T^{\Lambda}_{\lambda\mu'})(T^{\Lambda}_{\lambda\mu}|\widehat{A}|\rho_0) \end{aligned} \tag{8}$$

The signals from the $\mathcal{N}$ different experiments are multiplied by a set of weighting factors and added together. The total signal is given by

$$\bar{s}(t) = \sum_{j=0}^{\mathcal{N}-1} w_j s(j,t) \tag{9}$$

where w_j is the weighting factor used for the signal from the jth experiment.

Suppose now that the angles Ω_j and weights w_j are chosen so that the following condition is satisfied:

$$\sum_{j=0}^{\mathcal{N}-1} w_j D^{\lambda}_{\mu\mu'}(\Omega_j) = \delta_{\lambda 0}\delta_{\mu 0}\delta_{\mu' 0} \quad \text{for } 0 \leqslant \lambda \leqslant \lambda_{\max} \tag{10}$$

Eqs. (8)–(10) may be combined to obtain:

$$\bar{s}(t) \cong s_{00}(t) \tag{11}$$

which is the desired result.

The angle sets which satisfy the condition in Eq. (10) are now derived. The polar angles $\{\theta_{\mathrm{v}}(j_1), \phi_{\mathrm{v}}(j_1)\}$ describing the vertices of the regular polyhedra listed in Table 1 fulfill the following condition:

$$\sum_{j_1=0}^{\mathcal{V}-1} w_j D^{\lambda}_{\mu 0}(\phi_{\mathrm{v}}(j_1), \theta_{\mathrm{v}}(j_1), 0) = \delta_{\lambda 0}\delta_{\mu 0} \quad \text{for } 0 \leqslant \lambda \leqslant \lambda_{\max} \tag{12}$$

where the weights are uniform: $w_j = \mathcal{V}^{-1}$. The full condition in Eq. (10) is completed by allowing the third Euler angle γ_j to step around a circle in $\lambda_{\max} + 1$ steps, for every pair of polar angles $\{\theta_{\mathrm{v}}(j_1), \phi_{\mathrm{v}}(j_1)\}$. This leads to the following algorithm for the three Euler angles:

$$\begin{aligned} \alpha_j &= \phi_{\mathrm{v}}(j_1) \\ \beta_j &= \theta_{\mathrm{v}}(j_1) \\ \gamma_j &= \frac{2\pi j_2}{(\lambda_{\max}+1)} \end{aligned} \tag{13}$$

where j_1 and j_2 are derived from the index j through Eq. (2).

The rotation $\widehat{R}(\Omega_j)$, where the Euler angles $\Omega_j = \{\alpha_j, \beta_j, \gamma_j\}$ are given in Eq. (13), is implemented by using the phase specifications in Eq. (3). This may be shown through the following argument:

$$\begin{aligned} \widehat{R}_z(\alpha_j)\widehat{R}_y(\beta_j)\widehat{R}_z(\gamma_j) &= \widehat{R}_z(\alpha_j)\widehat{R}_x(-\pi/2)\widehat{R}_z(\beta_j)\widehat{R}_x(\pi/2)\widehat{R}_z(\gamma_j) \\ &= \widehat{R}_z(\alpha_j+\pi)\widehat{R}_x(\pi/2) \\ &\quad \times \widehat{R}_z(\beta_j-\pi)\widehat{R}_x(\pi/2)\widehat{R}_z(\gamma_j) \end{aligned} \tag{14}$$

The $\widehat{R}_z(\phi)$ rotations may be interpreted as overall radiofrequency phase shifts ϕ applied to all preceding pulse sequence elements, while the $\widehat{R}_x(\pi/2)$ rotations may be implemented by strong radiofrequency pulses of flip angle $\pi/2$.

It should be noted that the numbers of phase steps in Table 1 are not necessarily minimal. The construction principle in Eq. (13) handles the angles α_j and γ_j differently, and allows complete freedom in the starting angle for γ_j at each vertex. This suggests the existence of shorter solutions, and one has actually been discovered. We have recently shown that a set of 60 Euler angles derived from the vertices of the four-dimensional polytope called the 600-cell [26] has $\lambda_{\max} = 5$ and is formally equivalent to the 72-angle icosahedral set given in the last row of Table 1. This solution will be described elsewhere.

The phase cycles for isotropic filtering of an NMR signal are considerably shorter than those required for full spherical tensor analysis, given the same maximum rank. In general, spherical tensor analysis out to rank $\lambda_{\max}$ requires the use of Euler angle sets which integrate the Wigner functions perfectly out to rank $2\lambda_{\max}+1$, while isotropic filtering only requires the integration to be complete up to the rank $\lambda_{\max}$.

3. Application to singlet NMR

In some cases, singlet nuclear spin states have long decay time constants T_S which may exceed the spin-lattice relaxation time T_1 by an order of magnitude or more [12–21]. Such long-lived states have been used to study slow diffusional motion and chemical exchange [16,18]. Applications are anticipated for transporting and storing hyperpolarized spin order generated by chemical reactions of parahydrogen [19]. The existence of long-lived spin states in systems of more than two coupled spins has been discussed [15,20,21].

Several different pulse sequences have been demonstrated for populating nuclear singlet states in high magnetic field, starting from the Boltzmann population distribution in thermal equilibrium. Zero-quantum coherence [14,18] and two-spin longitudinal order [18] have both been used. However, none of the sequences known to date create a pure singlet population operator. There is always contamination with other spin order terms, even when all pulses are ideal. Some of these extra terms are zero-quantum in nature and cannot be removed by conventional phase cycling. As a result the slow singlet decay is contaminated with terms which decay more rapidly. This does not cause problems if the singlet decay is much slower than that of the other components, since the long-term behavior is then dominated by the singlet decay. However in less favorable circumstances, interference from other contributions hinders the estimation of the singlet decay time constant T_S.

The component of the NMR signal that passes through a singlet population term in the spin density operator may be isolated by isotropic filtration using a polyhedral phase cycle of the type presented above. This works because singlet states have total spin quantum number $I = 0$ and are invariant to rotations. The singlet population operator in a 2-spin-1/2 system is a spherical tensor operator of rank 0, as follows:

$$T_{00} = |S_0 >< S_0| = \frac{1}{2}(I_1^\alpha I_2^\beta + I_1^\beta I_2^\alpha - I_1^+ I_2^- - I_1^- I_2^+) \qquad (15)$$

where the singlet state of a 2-spin-1/2 system is defined by:

$$|S_0\rangle = \frac{1}{\sqrt{2}}(|\alpha\beta> - |\beta\alpha>) \qquad (16)$$

The unity operator, which represents a uniform population distribution, is also a spherical tensor operator of rank 0. By definition, any linear combination of the unity and the singlet population operator is also an isotropic spherical tensor operator. Note that the isotropic operator in Eq. (15) consists of a well-defined combination of zero-quantum coherence and population operators. Conventional phase cycling, which operators on the quantum order μ alone, cannot distinguish this term from isolated populations, or isolated zero-quantum coherences.

A spin ensemble of isolated 2-spin-1/2 systems only supports spin order terms with rank $\lambda_{max} \leqslant 2$. A 12-step tetrahedral phase cycle with $\lambda_{max} = 2$ is therefore sufficient for isotropic filtering of a 2-spin-1/2 NMR signal.

An illustrative case is provided by the proton spin system of citric acid (see Fig. 3a), which was studied before [15]. The proton NMR spectrum is shown in Fig. 3b. The proton $AA'BB'$ system of citric acid consists of two independent AB spin systems (one for each methylene group). Each AB system supports a long-lived singlet state. The strongly coupled nature of the AB spin systems makes it difficult to excite and observe singlet states cleanly.

The pulse sequences used to study the singlet states in citric acid are shown in Fig. 4. The conventional pulse sequence in Fig. 4a employs a sequence of two $\pi/2$ pulses, one π pulse, and three delays to populate the singlet state *via* zero-quantum coherence [14]. Other methods may also be used [18]. The singlet state is locked by a strong resonant rf field during the long interval τ_4 in order to prevent mixing with the short-lived triplet states. A further delay and a $\pi/2$ pulse generate a NMR signal which gives an antiphase signal pattern after Fourier transformation. Some examples are shown in Fig. 5(a–c). The amplitudes of the antiphase signals depend on the singlet population existing at the end of the spin-locking period. The decay of the singlet population may be studied by repeating the experiment for several values of the locking interval τ_4.

All results were obtained using 50 mg of citric acid, purchased from Sigma–Aldrich, and dissolved in 500 μl of DMSO-d_6. The solution was contained in a 5 mm Young-valve NMR tube and degassed by 6 pump-thaw cycles. The experiments were performed on a 9.4 T Varian Infinity+ spectrometer. The values of the delays used for singlet excitation and observation were $\tau_1 = 15.5$ ms, $\tau_2 = 4.5$ ms, $\tau_3 = 6.2$ ms and $\tau_5 = 6.2$ ms. The rf field during the spin-locking interval τ_4 provided a nutation fre-

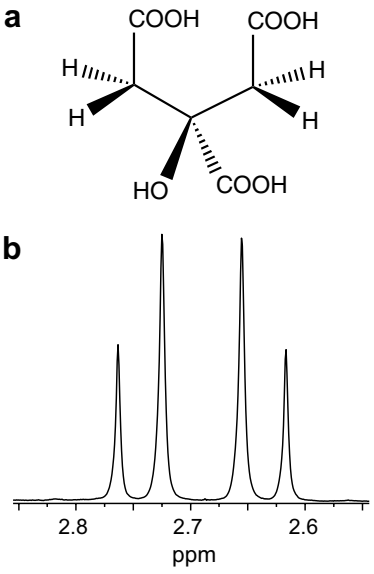

Fig. 3. (a) Molecular structure of citric acid. (b) Expanded region of the ^{1}H NMR spectrum of citric acid dissolved in DMSO-d_6 at room temperature.

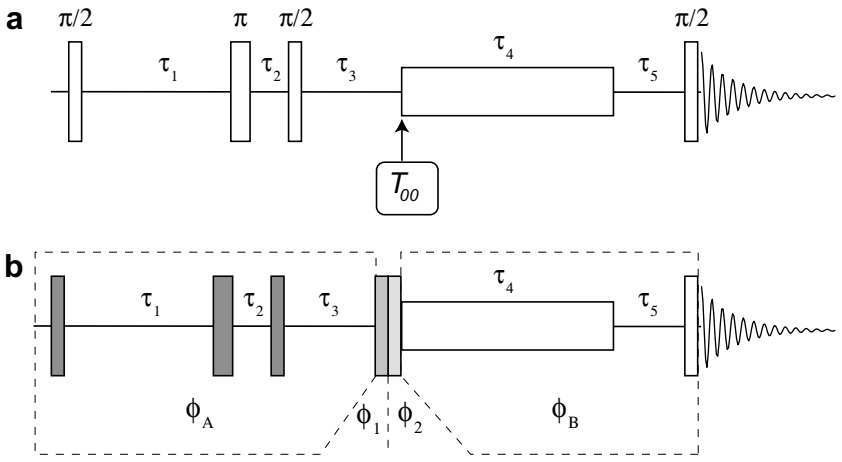

Fig. 4. (a) Pulse sequence for generating singlet population and observing its decay in the presence of a rf field. The singlet population is generated from zero-quantum coherence by the first three pulses and delays τ_1, τ_2 and τ_3. The singlet spin-locking is implemented for an interval τ_4. The singlet population is observed by converting it into observable magnetization by the delay τ_5 and the third $\pi/2$ pulse. (b) Implementation of isotropic filtering by inserting two strong $\pi/2$ pulses and subjecting the phases ϕ_A, ϕ_1, ϕ_2 and ϕ_B to a phase cycle.

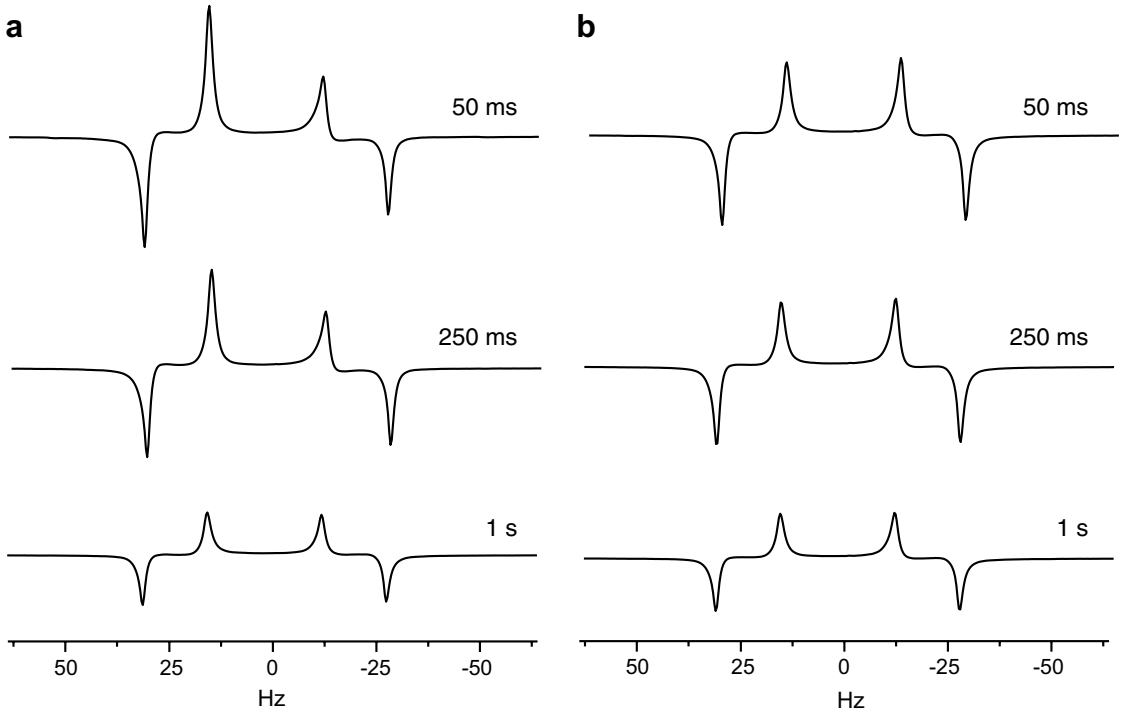

Fig. 5. (a) Spectral lineshapes obtained using the pulse sequence in Fig. 4a. (b) Spectral lineshapes obtained after isotropic filtration using the pulse sequence in Fig. 4b. The value of the spin-locking interval τ_4 is shown on the plots.

quency of 1.0 kHz and was applied at the center frequency of the AB signal pattern.

The spectral patterns obtained by Fourier transforming the signals generated by the pulse sequence in Fig. 4a for three different values of the locking interval τ_4 are shown in the left column of Fig. 5. As may be seen, the form of the spectra changes as τ_4 is increased. This indicates contamination of the signal at small values of τ_4 by a component with a different spectral signature and a relatively short decay time constant.

The experimental amplitude of the largest spectral peak (second from left) is plotted against the spin-locking time τ_4 in Fig. 6a. The best fit to a single-exponential decay is shown in the figure. The fit is imperfect, indicating the presence of more than one spin order term, with different decay time constants.

Isotropic filtering was implemented by inserting two $\pi/2$ pulses before the spin-locking interval, as shown in Fig. 4b. A 12-step tetrahedral phase cycle for the two $\pi/2$ pulses and the preceding pulse sequence block was

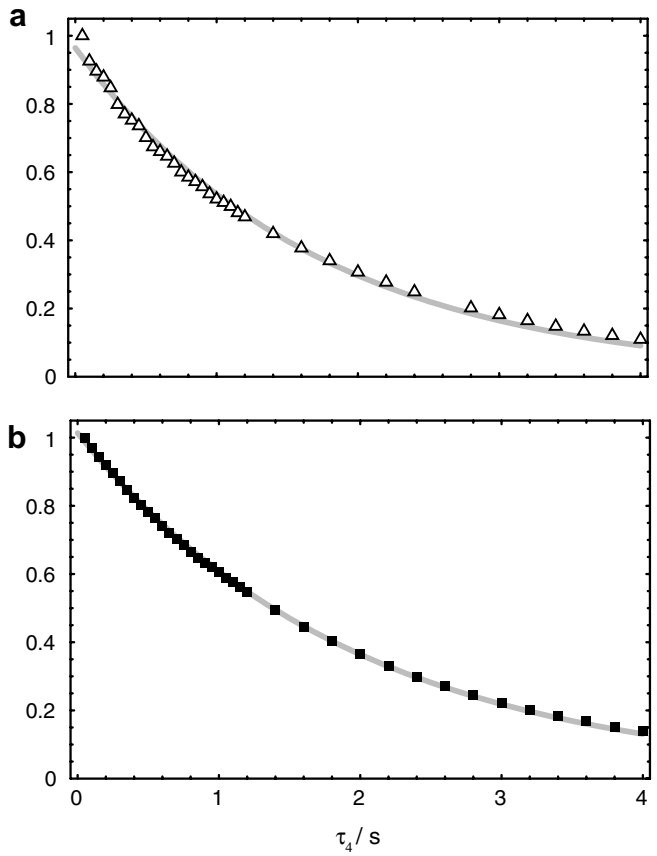

Fig. 6. (a) Experimental decays of the citric acid signal amplitude as a function of the spin-lock interval τ_4 for (a) the pulse sequence of Fig. 4a, and (b) the pulse sequence of Fig. 4b, implementing the isotropic filter. The best fits to single-exponential decays are shown by gray lines. Note the departure of the single-exponential fit from the experimental amplitudes in (a).

executed for every increment of τ_4, using the phase table given in Table 2.

The spectral patterns for the isotropically filtered signal are shown in the right column of Fig. 5. The spectra have a cleaner antiphase appearance, which is well-conserved as τ_4 is increased. The decay of the signal amplitudes is shown in Fig. 6b. The signal amplitudes are now fitted well by a single-exponential decay with time constant of 1.95 s. We conclude that the tetrahedral phase cycle has eliminated the interference from non-singlet terms, and that the singlet state has a decay time constant of $T_S = 1.95$ s in this system. This is about 5 times longer than the spin-lattice relaxation time $T_1 = 0.38$ s, as estimated by a conventional inversion-recovery experiment.

4. Conclusions

A technique for the isotropic filtering of NMR signals has been introduced and validated. Isotropic filtering is implemented by introducing two strong $\pi/2$ pulses into the pulse sequence at the time point of interest, and subjecting these two pulses and the preceding ones to a phase cycle. The phase angles are derived from the vertices of a regular polyhedron. In the most economical version, a 12-step tetrahedral phase cycle is used. The method is general and may be applied to any pulse sequence. In this report, isotropic filtering is used to isolate NMR signals passing through the long-lived singlet state of citric acid in solution, allowing an accurate measurement of the singlet decay, even in the presence of interference from other signal components. The experiment is likely to be useful for filtering out the signals from localized singlet states in biomolecules [18], suppressing the numerous signals from other species.

The procedures described in this paper may be adapted to other situations, for example the efficient computation of powder averages [23,24], and the averaging of spatial interaction tensors in the NMR of quadrupolar nuclei [27,28].

Acknowledgments

This research was supported by the EPSRC (UK). The authors thank Geoffrey Bodenhausen and Mattias Edén for comments on the text.

References

[1] R.R. Ernst, G. Bodenhausen, A. Wokaun, Principles of Nuclear Magnetic Resonance in One and Two Dimensions, Clarendon Press, Oxford, 1987.
[2] J. Keeler, Understanding NMR Spectroscopy, Wiley, Chichester, 2005.
[3] M.H. Levitt, P.K. Madhu, C.E. Hughes, Cogwheel Phase Cycling, J. Magn. Reson. 155 (2002) 300–306.
[4] A. Jerschow, R. Kumar, Calculation of coherence pathway selection and cogwheel cycles, J. Magn. Reson. 160 (2003) 59–64.
[5] N. Ivchenko, C.E. Hughes, M.H. Levitt, Application of cogwheel phase cycling to sideband manipulation experiments in solid-state NMR, J. Magn. Reson. 164 (2003) 286–293.
[6] G. Zuckerstätter, N. Müller, Coherence pathway selection by cogwheel phase cycling in liquid-state NMR, Concepts Magn. Reson. 30A (2007) 81–99.
[7] N. Ivchenko, C.E. Hughes, M.H. Levitt, Multiplex phase cycling, J. Magn. Reson. 160 (2003) 52–58.
[8] D. Suter, J.G. Pearson, Experimental classification of multi-spin coherence under the full rotation group, Chem. Phys. Lett. 144 (1988) 328.
[9] J.D. van Beek, M. Carravetta, G.C. Antonioli, M.H. Levitt, Spherical tensor analysis of nuclear magnetic resonance signals, J. Chem. Phys. 122 (2005) 24510.
[10] G.J. Bowden, W.D. Hutchison, Tensor operator formalism for multiple-quantum NMR. 1. Spin-1 nuclei, J. Magn. Reson. 67 (1986) 403–414.
[11] B.C. Sanctuary, T.K. Halstead, Multipole NMR Adv. Magn. Opt. Reson. 15 (1990) 80.
[12] M. Carravetta, O.G. Johannessen, M.H. Levitt, Beyond the T_1 limit: singlet nuclear spin states in low magnetic fields, Phys. Rev. Lett. 92 (2004) 153003.
[13] M. Carravetta, M.H. Levitt, Theory of long-lived nuclear spin states in solution nuclear magnetic resonance. I. Singlet states in low magnetic field, J. Chem. Phys. 122 (2005) 214505.
[14] M. Carravetta, M.H. Levitt, Long-lived nuclear spin states in high-field solution NMR, J. Am. Chem. Soc. 126 (2004) 6228–6229.
[15] G. Pileio, M. Concistrè, M. Carravetta, M.H. Levitt, Long-lived nuclear spin states in the solution NMR of four-spin systems, J. Magn. Reson. 182 (2006) 353–357.

[16] S. Cavadini, J. Dittmer, S. Antonijevic, G. Bodenhausen, Slow diffusion by singlet state NMR, J. Am. Chem. Soc. 127 (2005) 15744–15748.
[17] K. Gopalakrishnan, G. Bodenhausen, Lifetimes of singlet-states under coherent off-resonance irradiation in NMR spectroscopy, J. Magn. Reson. 182 (2006) 254–259.
[18] R. Sarkar, P.R. Vasos, G. Bodenhausen, Singlet-state exchange NMR spectroscopy for the study of very slow dynamic processes, J. Am. Chem. Soc. 129 (2007) 328–334.
[19] T. Jonischkeit, U. Bommerich, J. Stadler, K. Woelk, H.G. Niessen, J. Bargon, Generating long-lasting ^{1}H and ^{13}C hyperpolarization in small molecules with parahydrogen-induced polarization, J. Chem. Phys. 124 (2006) 201109.
[20] G. Pileio, M.H. Levitt, J-stabilization of singlet states in the solution NMR of multiple-spin system, J. Magn. Reson. 187 (2007) 141–145.
[21] E. Vinogradov, A.K. Grant, Long lived states in solution NMR: selection rules for intramolecular dipolar relaxation in low magnetic fields, J. Magn. Reson. 188 (2007) 176–182.
[22] M. Carravetta, A. Danquigny, S. Mamone, F. Cuda, O.G. Johannessen, I. Heinmaa, K. Panesar, R. Stern, M.C. Grossel, A.J. Horsewill, A. Samoson, M. Murata, Y. Murata, K. Komatsu, M.H. Levitt, Solid-state NMR of endohedral hydrogen-fullerene complexes, Phys. Chem. Chem. Phys. 9 (2007) 4879.
[23] M. Edén, M.H. Levitt, Computation of orientational averages in solid state NMR by Gaussian spherical quadrature, J. Magn. Reson. 132 (1998) 220–239.
[24] B. Stevensson, M. Edén, Efficient orientational averaging by the extension of Lebedev grids via regularized octahedral symmetry expansion, J. Magn. Reson. 181 (2006) 162–176.
[25] J. Jeener, Superoperators in magnetic resonance, Adv. Magn. Reson. 10 (1982) 1–51.
[26] H.S.M. Coxeter, Regular Polytopes, Macmillan, New York, 1963.
[27] A. Samoson, E. Lippmaa, A. Pines, High-resolution solid-state NMR averaging of second-order effects by means of a double rotor, Mol. Phys. 65 (1988) 1013–1018.
[28] B.F. Chmelka, A. Pines, Some developments in nuclear magnetic resonance of solids, Science 246 (1989) 71–77.